Continuously Tunable Charge in Andreev Quantum Dots

I.A. Sadovskyy[a], G.B. Lesovik[a], and G. Blatter[b]

[a] L.D. Landau Institute for Theoretical Physics RAS, 119334 Moscow, Russia and
[b] Theoretische Physik, Schafmattstrasse 32, ETH-Zurich, CH-8093 Zürich, Switzerland

(Dated: February 5, 2008)

We show that a quantum dot connected via tunnel barriers to superconducting leads traps a continuously tunable and hence fractional charge. The fractional charge on the island is due to particle-hole symmetry breaking and can be tuned via a gate potential acting on the dot or via changes in the phase difference across the island. We determine the groundstate, equilibrium, and excitation charges and show how to identify these quantities in an experiment.

PACS numbers: 73.21.La 74.45.+c 74.78.Na

The superconducting phase φ is usually associated with a dissipation-free flow of current; a phase twist by 2π within a bulk superconductor drives a magnetic vortex [1] and a phase drop φ across a junction drives a Josephson current [2]. Only much later it has been recognized that vortices carry a (small) charge as well [3], an effect which is due to particle-hole symmetry breaking. In this letter, we show that particle-hole asymmetry also generates a localized charge in a metallic quantum dot coupled to a superconducting loop, a so-called Andreev quantum dot [4], see Fig. 1(a). This charge is continuously tunable (and hence fractional) through the gate potential V_g or via the phase bias φ across the dot. It manifests itself for the (even parity) ground- and doubly-occupied excited states, while the (odd parity) singly-occupied excited state exhibits an integer charge, see Fig. 1(c); as a corollary, the excitation charges are non-integer as well. The fractional charge can be observed via measurement of the associated telegraph noise signal due to the stochastic occupation of the Andreev states or through its dependence on the flux threading the loop. The latter provides a realization of a flux-to-charge converter allowing to make use of the device as a magnetic-flux detector.

A tunable charge in a mesoscopic setup, a ring with a (nearby or interrupting) quantum dot, has been discussed in Refs. [7, 8]; the origin of this fractional charge is easily understood in terms of the extended nature of the wave function, with only a fraction localized on the dot. This contrasts with the fractional charge discussed here, where the 'missing' part is completely delocalized in the nearby superconducting condensate. Our charge then reminds about the fractional charge associated with excitations in a superconductor which has been discussed in the context of charge relaxation [5] (or branch imbalance [6]) in non-equilibrium superconductivity; there, too, the missing charge is 'dissolved' in the superconducting condensate. In the following, we first discuss in detail the origin of the tunable charge which we then determine quantitatively. We discuss quantum fluctuations in the trapped charge as well as corrections due to weak Coulomb interactions, see Ref. [9] for a discussion

of strong Coulomb effects and the Kondo effect in an Andreev dot. We end with a discussion of telegraph noise allowing to detect the fractional charge.

In superconducting mesoscopic devices the phenomenon of Andreev scattering [10] plays a central role: electrons (holes) incident from a normal metal (N) with
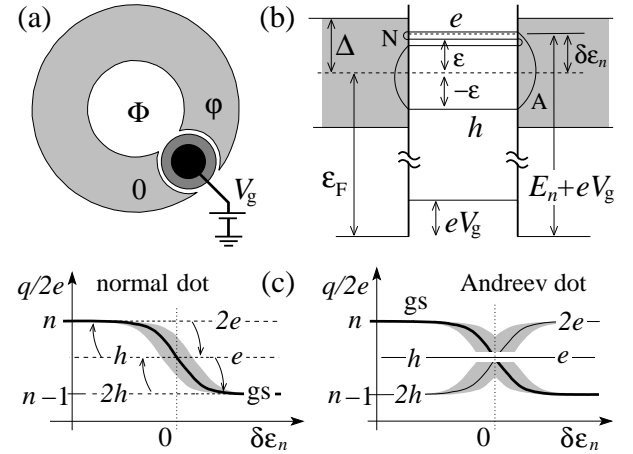

FIG. 1: (a) Andreev dot (SINIS) embedded in a superconducting ring. Tuning of flux Φ or gate potential V_g serves to modify the charge on the dot. (b) The mixing of Andreev- and normal scattering at an SIN boundary leads to particle-hole symmetry breaking and to the appearance of a fractional charge on the dot. The phenomenon shows up in the vicinity of a resonance in the associated NININ device, here an electron type resonance, where the electron quasi-particle is multiply reflected while the hole component is not. (c) Charge trapped on normal- and Andreev dots versus position of resonance $\delta\varepsilon_n$; shown are the ground-state (gs) and single-particle excited-state charges for the singly and doubly occupied situation. gs: as the resonance passes the Fermi level, a charge $2e$ is pushed out of the dot over a width Γ; the shaded areas indicate the importance of quantum fluctuations. Dashed lines (normal dot) indicate electron- and hole- type resonances; the associated trapped charges decay rapidly to the ground state charge (arrows). These resonances are transformed into eigenstates in the Andreev dot; they carry integer charge if occupied once (odd-parity) and a fractional charge when occupied twice (even-parity).

energies $|E - \varepsilon_{\mathrm{F}}| < \Delta$ and scattering off a superconductor (S) are reflected as holes (electrons) with a Cooper-pair entering (leaving) the superconductor (here, ε_{F} and Δ denote the Fermi energy and the superconducting gap). In an SNS junction, electrons convert to holes at one NS boundary and back to electrons at the opposite NS contact, thus generating a particle-hole symmetric uncharged bound state (we ignore a small electron-hole symmetry breaking of order $\Delta/\varepsilon_{\mathrm{F}}$). When the NS interfaces are augmented by thin insulating layers I in an SINIS junction, the particles in the normal-metal region undergo imperfect Andreev scattering at the NIS boundaries with mixed Andreev- and normal scattering processes; the resulting Andreev levels involve unequal electron- and hole-like components and hence particle-hole symmetry is broken, see Fig. 1(b). Alternatively, the Andreev state can be understood as deriving from normal resonances in the associated NININ structure — replacing the normal leads by superconducting ones, a resonance residing in the gap region transforms into a sharp Andreev level with predominantly electron- (resonance above ε_{F}) or hole character (resonance below ε_{F}). The properties of these trapped Andreev states are easily tuned, either through shifts in their position within the gap via changing gate bias V_g or via changes in the phase φ across the superconducting banks.

The Andreev states give rise to new opportunities for tunable Josephson devices, e.g., the Josephson transistor [11, 12]; here, we are interested in their charging properties. Below, we consider small islands with a large separation δ_n of resonances in the associated NININ problem, $\delta_n > \Delta$, such that a single Andreev level is trapped within the gap region. Such Andreev dots have recently been fabricated by coupling carbon nanotubes to superconducting banks [13, 14], with the main focus on the competition between the Kondo effect and superconductivity [13]. We are interested in sufficiently well isolated islands with a small width Γ_n of the associated NININ resonance, $\Gamma_n < \Delta$. Also, we wish to neglect charging effects in our first analysis here and hence demand that the Coulomb energy is small, $E_{\mathrm{C}} < \Gamma_n$. In summary, our device operates with energy scales $E_{\mathrm{C}} < \Gamma_n < \Delta < \delta_n$, a situation which can be generated in the lab, see our estimates below. In what follows, we determine the charge configuration of the ground- and excited states versus V_g and φ, find the thermal equilibrium charge and discuss the excitation dynamics of the Andreev states (due to elastic and Coulomb interactions) providing the characteristics of the telegraph noise in the charge state of the dot.

The resonances in the NININ setup derive from the eigenvalue problem $H_0 \Psi = E \Psi$ with $H_0 = -\hbar^2 \partial_x^2 / 2m + U(x) - \varepsilon_{\mathrm{F}}$ and the potential $U(x) = U_{\mathrm{ps}}(x+L/2) + U_{\mathrm{ps}}(x - L/2)] + eV_g \Theta(L/2 - |x|)]$ describing two point-scatterers (with transmission and reflection coefficients $\sqrt{T} e^{i\chi^t}$ and $\sqrt{R} e^{i\chi^r}$) and the effect of the gate potential V_g, which we

assume to be small as compared to the particle's energy E (measured from the band bottom in the leads), $eV_g \ll E$. Resonances then appear at energies $E_n = \varepsilon_L (n\pi - \chi^r)^2$; they are separated by $\delta_n = (E_{n+1} - E_{n-1})/2 \approx 2E_n/n$ and are characterized by the width $\Gamma_n = T\delta_n / \pi\sqrt{R}$, where $\varepsilon_L = \hbar^2 / 2mL^2$. The bias V_g shifts the resonances by eV_g; we denote the position of the n-th resonance relative to ε_{F} by $\delta\varepsilon_n = E_n + eV_g - \varepsilon_{\mathrm{F}}$, see Fig. 1(b).

We go from a normal- to an Andreev dot by replacing the normal leads with superconducting ones. In order to include Andreev scattering in the SINIS setup we have to solve the Bogoliubov-de Gennes equations (we choose states with $\varepsilon \geq 0$, see Fig. 1(b))

$$\begin{bmatrix} H_0 & \Delta(x) \\ \Delta^*(x) & -H_0 \end{bmatrix} \begin{bmatrix} u_n(x) \\ v_n(x) \end{bmatrix} = \varepsilon_n^{\mathrm{A}} \begin{bmatrix} u_n(x) \\ v_n(x) \end{bmatrix}, \tag{1}$$

with the pairing potential $\Delta(x) = \Delta[\Theta(-x - L/2)e^{-i\varphi/2} + \Theta(x - L/2)e^{i\varphi/2}]$; $u_n(x)$ and $v_n(x)$ are the electron- and hole-like components of the wave function. The discrete states trapped below the gap derive from the quantization condition (in Andreev approximation; the bar '$\bar{\cdot}$' and indices '$\pm$' refer to scattering probabilities and phases for the NININ setup and energies $\varepsilon_{\mathrm{F}} \pm \varepsilon$)

$$\cos(S_+ - S_- - 2\alpha) = \sqrt{\bar{R}_+ \bar{R}_-} \cos\beta + \sqrt{\bar{T}_+ \bar{T}_-} \cos\varphi. \tag{2}$$

The phase $\alpha = \arccos(\varepsilon_n^{\mathrm{A}}/\Delta)$ is due to Andreev scattering and the phases $S_\pm = \chi_\pm^t + k_\pm L$, $k_\pm = \sqrt{2m(\varepsilon_{\mathrm{F}} \pm \varepsilon)}/\hbar$ account for the propagation across the island; for symmetric barriers the phase $\beta = (\bar{\chi}_+^t - \bar{\chi}_+^r) - (\bar{\chi}_-^t - \bar{\chi}_-^r)$ is a multiple of π and produces a smooth function $\sqrt{\bar{R}_+ \bar{R}_-} \cos\beta$ changing sign at every resonance [12, 15].

The solution of (2) is straightforward and provides the spectrum shown in Fig. 2(a). A small dot $L \lesssim \xi$ (ξ the superconducting coherence length) results in a single Andreev state which lives near (but below) the gap Δ when the dot is tuned far off resonance with $|\delta\varepsilon_n| \gg \Delta$, $\varepsilon_n^{\mathrm{A}} \approx \Delta(1 - \Gamma_n^2 / 8\delta\varepsilon_n^2)$; when the resonance resides in the gap region, $|\delta\varepsilon_n| < \Delta$, the associated Andreev level approaches the Fermi energy ε_{F} linearly,

$$\varepsilon_n^{\mathrm{A}} \approx (1 - \Gamma_n/2\Delta)|\delta\varepsilon_n|, \tag{3}$$

where we have assumed $\Gamma_n \ll \Delta$. As $\varepsilon_n^{\mathrm{A}}$ drops below the resonance width Γ_n the Andreev state becomes sensitive to the phase difference φ across the junction,

$$\varepsilon_n^{\mathrm{A}} \approx (1 - \Gamma_n/2\Delta)\sqrt{\delta\varepsilon_n^2 + (\Gamma_n/2)^2 \cos^2(\varphi/2)}. \tag{4}$$

The resonances above Δ follow closely the normal resonances ε_n, see Fig. 2(a).

The Andreev state at $\varepsilon_n^{\mathrm{A}}$ carries a nontrivial charge which we find as the expectation value of the charge operator (for the space interval $[-a, a]$) $Q^a \equiv e \int_{-a}^{a} dx \sum_{\sigma=\pm 1} \Psi_\sigma^\dagger(x) \Psi_\sigma(x)$ with $\Psi_\sigma(x) = \sum_n [u_n(x)\alpha_{n,\sigma} + \sigma v_n^*(x)\alpha_{n,-\sigma}^\dagger]$ and $\alpha_{n,\sigma}$, $\alpha_{n,\sigma}^\dagger$ the usual

Bogoliubov operators; the $\sum_n$ includes localized and extended states. Defining the quantities $q_{n,u}^a \equiv \int_{-a}^{a} dx\, e|u_n(x)|^2$ and $q_{n,v}^a \equiv \int_{-a}^{a} dx\, e|v_n(x)|^2$ (with the normalization $q_{n,u}^\infty + q_{n,v}^\infty = e$), we obtain the thermal equilibrium charge (we subtract the charge $2e(n-1)$ due to filled resonances and continuum states)

$$q_{n,\mathrm{eq}}^a = 2f(\varepsilon_n^A)\, q_{n,u}^a + 2[1 - f(\varepsilon_n^A)]\, q_{n,v}^a; \qquad (5)$$

setting the Fermi function $f(\varepsilon)$ to zero we obtain the ground state charge $q_{n,\mathrm{gs}}^a \equiv \langle 0|Q^a|0\rangle = 2q_{n,v}^a$. The excitation charge (of one spin state $|\sigma\rangle$) assumes the value

$$q_{n,\mathrm{ex}}^a \equiv \langle\sigma|Q^a|\sigma\rangle - \langle 0|Q^a|0\rangle = q_{n,u}^a - q_{n,v}^a. \qquad (6)$$

These charges are localized around the dot, either strictly within the region $[-L/2.L/2]$ as for the excitation charge $q_{n,\mathrm{ex}}^\infty = q_{n,\mathrm{ex}}^{L/2}$ or with an additional extension of size $\sim \xi$ around the dot carrying a small weight [17], $q_{n,\mathrm{eq}}^\infty \approx q_{n,\mathrm{eq}}^{L/2}$ (hence, the fractional charge is *not* due to a missing part of a wave function). The excitation charge can be directly obtained from the voltage dispersion of the Andreev state, $q_{n,\mathrm{ex}}^{L/2} = \partial_{V_g}\varepsilon_n^A$; combining this with the normalization condition, the other charges $q_{n,\mathrm{eq}}^\infty$ and $q_{n,\mathrm{gs}}^\infty$ follow immediately. The expressions (3) and (4) for the position ε_n^A provides the excitation charge,

$$q_{n,\mathrm{ex}}^{L/2} \approx \begin{cases} \dfrac{e\,(1 - \Gamma_n/2\Delta)\delta\varepsilon_n}{\sqrt{\delta\varepsilon_n^2 + (\Gamma_n/2)^2\cos^2(\varphi/2)}}, & \delta\varepsilon_n < \Gamma_n, \\[2mm] \mathrm{sign}(\delta\varepsilon_n)\,e\,(1 - \Gamma_n/2\Delta), & \delta\varepsilon_n < \Delta, \\[2mm] \mathrm{sign}(\delta\varepsilon_n)e\,\Delta\Gamma_n^2/4\delta\varepsilon_n^3, & \Delta < \delta\varepsilon_n. \end{cases} \qquad (7)$$
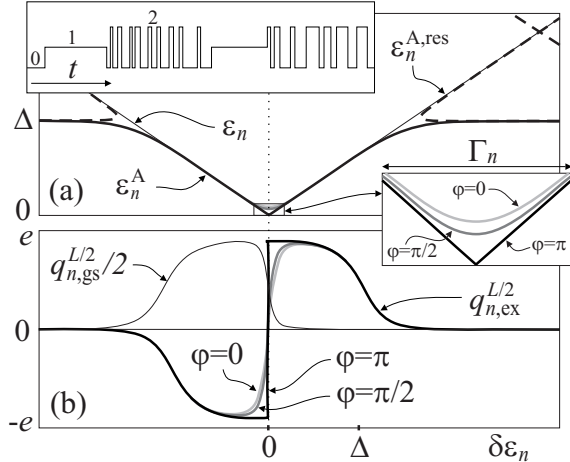

FIG. 2: (a) Bound state ε_n^A (thick solid lines) and resonances $\varepsilon_n^{A,\mathrm{res}}$ (dashed lines) in the Andreev dot versus position $\delta\varepsilon_n$ of the normal state resonance (tuned via the gate potential V_g); we choose $\Gamma_n = 0.2\Delta$. Also shown are the normal resonances ε_n (thin solid line) and the dependence on the phase difference φ across the dot (inset). (b) Charges $q_{n,\mathrm{ex}}^{L/2}$ and $q_{n,\mathrm{gs}}^{L/2}$. Top inset: structure of telegraph noise with long periods of ground state (0) and singly occupied (1) states and the ground state trace interrupted by fast doubly excited states (2).

The full numerical result is shown in Fig. 2(b): the charge rises linearly (with slope $\approx 2e/\Gamma_n\cos(\varphi/2)$; note the sharp change in charge for a π-tuned Andreev dot at $\varphi = \pi$) as the normal resonance crosses the Fermi level and then saturates at a value $e\,(1 - \Gamma_n/2\Delta)$. As the normal resonance leaves the gap region, $|\delta\varepsilon_n| > \Delta$, the charge $q_{n,\mathrm{ex}}^{L/2}$ vanishes $\propto \Delta\Gamma_n^2/\delta\varepsilon_n^3$. We see, that tunable fractional and localized ground state- and excitation charges appear on the Andreev dot each time a normal resonance crosses the Fermi level; this is the main result of our paper. Note that the addition of the (fractional) ground-state- and excitation charges conspires to produce the integer charge of the singly-occupied odd-parity excited state, $\langle\sigma|Q^{L/2}|\sigma\rangle = q_{n,u}^{L/2} + q_{n,v}^{L/2} \approx e$.

The above non-trivial charges are a consequence of the broken particle-hole symmetry and result from a super-position of states with definite integer charge, electron- and hole-like. As a result, the charges will undergo quantum fluctuations which are quantified by the variance $\delta q^a \equiv [\langle(Q^a)^2\rangle - \langle Q^a\rangle^2]^{1/2}$. Here, we are interested in the charge fluctuations of the ground- and singly/doubly excited states $|0\rangle$, $|\pm 1\rangle$, and $|2\rangle$; with $\langle\nu|(Q^a)^2|\nu\rangle = \sum_\mu |\langle\nu|Q^a|\mu\rangle|^2$ the determination of δq^a involves the calculation of matrix elements $\langle\nu|Q^a|\mu\rangle$. A detector will measure the charge over some time interval τ such that the relevant charge is given by the time average $\bar{Q}^a \equiv \int_0^\tau (dt/\tau)Q^a(t)$; as a result, only matrix elements connecting states with energy difference less than $\hbar/\tau$ have to be considered; assuming typical measurement frequencies $1/\tau \ll \Delta/\hbar$, we can restrict the sum over intermediate states $|\mu\rangle$ to the four states $|0\rangle$, $|\pm 1\rangle$, $|2\rangle$. The only relevant matrix element then is $\langle 0|Q^a|2\rangle = 2e\int_{-a}^{a} dx\, u_n(x)v_n(x)$ which is of order e. Hence, the charges of the singly-occupied states $|\pm 1\rangle$ do not fluctuate, while the charges of the ground- and doubly-excited states fluctuate strongly, see Fig. 1(c).

Next, let us comment on the effects of Coulomb interactions. Two important issues are the screening of the dot's charge and the mixing between charge states. Screening due to additional charge-flow to and from the Andreev dot is governed by the density of states. The relevant energy scale is given by the distance δ_n between resonances (as these carry large local charges) and hence on-dot charge screening is irrelevant if $E_C \ll \delta_n$. Mixing of states is again governed by the matrix elements $\langle\nu|(Q^a)^2|\nu\rangle$; restricting the analysis to the four states $|0\rangle$, $|\pm 1\rangle$, $|2\rangle$, we find that mixing occurs between the ground- and doubly-excited states but is small if $E_C \ll \varepsilon_n^A$. The energy scale $E_C \approx e^2/2C$ can be estimated via the capacitance $C \approx \epsilon L$ of the Andreev dot with ϵ the dielectric constant; on the other hand, the distance between resonances $\delta_n = hv_F/2L$ depends linearly on L, too. The crucial dimensionless device parameter is the ratio $\delta_n/E_C = hv_F\epsilon/e^2$; assuming typical values $\epsilon \sim 10$ and $v_F \sim 10^6$ m/s, we obtain a ratio $\delta_n/E_C \approx 30$, allowing for a sequence of energies $E_C < \Gamma_n < \Delta < \delta_n$ as

required in our setup. In Ref. [14] an Andreev dot in the form of a nanotube with $L \approx 500$ nm has been studied, that corresponds to a charging energy $E_{\rm C}$ of order one Kelvin, hence the above inequalities can be satisfied in a realistic device.

The fractional charge of excitations can be detected by various means; here, we discuss its observation through the measurement of the telegraph noise which arises due to the thermal occupation of states (we denote temperature by θ and set $k_{\rm B} = 1$). The noise pattern involves the three states $|\pm 1\rangle$ and $|2\rangle$; these states are filled and emptied through phonon absorption and emission processes [18]; in addition, fluctuations of the gate potential provide a competing channel. Two types of processes contribute to the telegraph noise, those coupling the ground- and singly-occupied states with rates γ_{01} and $\gamma_{10} = \gamma_{01} \exp(\varepsilon/\theta)$, and those coupling the ground- and doubly-occupied states with rates γ_{02} and $\gamma_{20} = \gamma_{02} \exp(2\varepsilon/\theta)$ (we introduce the shorthand $\varepsilon = \varepsilon_n^{\rm A}$; the rates connecting $|\pm 1\rangle$ and $|2\rangle$ agree with the single-particle rates, $\gamma_{01} = \gamma_{12}$ and $\gamma_{10} = \gamma_{21}$). The transitions $0 \leftrightarrow 1$ involve a second quasiparticle in the continuum with energy $E > \Delta$.

The rates γ_{01} and γ_{02} are derived from Fermi's Golden Rule with the perturbation given by the electron-phonon interaction $H = g \int dx\, n_e (\partial_x u)$ with u the displacement, n_e the electronic density, and g the electron-phonon coupling assuming values of order 1 eV (we consider one-dimensional modes for both electrons and phonons); an alternative channel is provided by the fluctuating gate potential with $H = \int dx\, e\, n_e V_g$. Concentrating on elastic modes, the determination of γ_{02} is straightforward and a simple estimate provides the result ($N_{2\varepsilon}$ is the Bose factor for the phonon state, a and $k > 1/L$ denote the lattice constant and the phonon wave number) $\gamma_{02} \sim (g^2/\hbar m v_{\rm F}^2)(a/kL^2) N_{2\varepsilon}$. As $k < 1/L$, we enter the zero-dimensional case and the result crosses over to $\gamma_{02} \sim (g^2/\hbar m v_{\rm F}^2)\, ak\, N_{2\varepsilon}$. On the other hand, fluctuations of the gate potential contribute the rate $\tilde{\gamma}_{02} \sim (e^2/\hbar C) N_{2\varepsilon}$. The numerical estimate with $g \sim 1$ eV, $m v_{\rm F}^2 \sim 1$ eV, and $L \approx 500$ nm provides the result $\gamma_{02} \sim 10^{12}$ s$^{-1} N_{2\varepsilon}$ at $k \sim 1/L$, which has to be compared with the Coulomb term $\tilde{\gamma}_{02} \sim 10^{11} N_{2\varepsilon}$ s^{-1}.

The calculation of the rate γ_{01} involves an additional sum over continuum states which is dominated by energies $E \sim \Delta$; here, we estimate the rate for the simultaneous occupation of the Andreev state and a continuum state under phonon absorption and find $\gamma_{01} \sim (g^2 T/\hbar m v_{\rm F}^2)(as/Lv_{\rm F})\sqrt{\theta/\Delta}\, e^{-\Delta/\theta}[1 + e^{-\varepsilon/\theta}]$, where s denotes the speed of sound. Note that $kL \sim \Delta L/\hbar s \gg 1$ in the present case. Fluctuations of the gate potential contribute with a rate $\tilde{\gamma}_{01} \sim \hbar^{-1}(e^2/C)\sqrt{\theta/\Delta}\, e^{-\Delta/\theta}[1 + e^{-\varepsilon/\theta}]$; using typical parameters $\theta \approx 0.1\Delta \approx 1$ K and $v_{\rm F}/s \sim 10^3$, we obtain numerical results of order $\gamma_{01} \sim 10^{10}$s$^{-1} T \exp(-\Delta/\theta)$ and $\tilde{\gamma}_{01} \sim 10^{11}s^{-1} \exp(-\Delta/\theta)$ due to elastic and Coulomb interactions, respectively [19].

Summarizing, we find that the processes $0 \leftrightarrow 2$ are always fast, while the $0 \leftrightarrow 1$ transitions involve the exponential factor $\exp(-\Delta/\theta)$, allowing us to reduce the rate γ_{01} dramatically by lowering the temperature. Hence, the $0 \leftrightarrow 1$ processes can be effectively separated from the $0 \leftrightarrow 2$ transitions, an effect which can be exploited in the experimental detection of the fractional charge.

Given today's performance of single electron transistors (SET) operating with a sensitivity of $\sim 10^{-5} e/\sqrt{\rm Hz}$ at frequencies $f < 10^9$ Hz [20], the telegraph noise due to the thermal population of the Andreev state may be observable and thus the fractional charge on the Andreev dot may be measured. However, the processes $0 \leftrightarrow 2$ may well be too fast, beyond today's time resolution of a SET. In this case we suggest two alternative schemes for the measurement of the excitation charge: i) Measuring the time averaged equilibrium charge $q_{n,\rm eq}^a$ once at high temperatures, $q_{n,\rm eq}^a(\theta \gg \varepsilon) = q_{n,u}^a + q_{n,v}^a$, and another time at low temperatures, $q_{n,\rm eq}^a(\theta \ll \varepsilon) = 2q_{n,v}^a$, their difference provides the excitation charge $q_{n,\rm ex}^a = q_{n,u}^a - q_{n,v}^a$. ii) A measurement at low temperatures resolving the slow $0 \leftrightarrow 1$ transitions and averaging over the fast $0 \leftrightarrow 2$ processes, see Fig. 2, measures the following (average) charges: given the occupation probabilities $p_0 = (1 - f_\varepsilon)^2$, $p_1 = 2f_\varepsilon(1 - f_\varepsilon)$, and $p_2 = f_\varepsilon^2$, the average over the rapidly fluctuating regimes involving the states 0 and 2 provides the charge $\langle q_n^a \rangle_{0,2} \approx 2q_{n,v}^a + 2f_\varepsilon^2 q_{n,\rm ex}^a$, while the singly charged regime appears with the trivial average $\langle q_n^a \rangle_1 = q_{n,v}^a + q_{n,u}^a$. At low temperatures we have $f_\varepsilon \ll 1$ and the difference $\langle q_n^a \rangle_1 - \langle q_n^a \rangle_{0,2} \approx q_{n,u}^a - q_{n,v}^a$ gives $q_{n,\rm ex}^a$.

In conclusion, we have discussed the peculiar properties of the trapped charge on an Andreev dot. We have found continuously tunable fractional and fluctuating charges for the ground- and doubly-excited states, while the odd-parity singly-occupied state exhibits an integer charge. The transition dynamics of these states allows to observe these charges in the telegraph noise.

---

[1] A.A. Abrikosov, Sov. Phys. JETP **5**, 1174 (1957).

[2] B.D. Josephson, Physics Letters **1**, 251 (1962).

[3] D.I. Khomskii and A. Freimuth, Phys. Rev. Lett. **75**, 1384 (1995); G. Blatter, M. Feigelman, V. Geshkenbein, A. Larkin, and A. van Otterlo, Phys. Rev. Lett. **77**, 566 (1996).

[4] N.M. Chtchelkatchev and Yu.V. Nazarov, Phys. Rev. Lett. **90**, 226806 (2003).

[5] C.J. Pethick and H. Smith, Annals of Physics **119**, 133 (1979).

[6] G.E. Blonder, M. Tinkham, and T.M. Klapwijk, Phys. Rev. B **25**, 4515 (1982).

[7] M. Büttiker and C.A. Stafford, Phys. Rev. Lett. **76**, 495 (1996).

...

[8] P.S. Deo, P. Koskinen, and M. Manninen, Phys. Rev. B **72**, 155332 (2005).

[9] A.V. Rozhkov and D.P. Arovas, Phys. Rev. B **62**, 6687 (2000).

[10] A.F. Andreev, Sov. Phys. JETP **19**, 1228 (1964).

[11] H. van Houton, Appl. Phys. Lett. **58**, 1326 (1991); G. Wendin and V.S. Shumeiko, Superlattices and Microstructures **20**, 569 (1996);

[12] D.D. Kuhn, N.M. Chtchelkatchev, G.B. Lesovik, and G. Blatter, Phys. Rev. B **63**, 054520 (2001).

[13] M.R. Buitelaar, T. Nussbaumer, and C. Schönenberger, Phys. Rev. Lett. **89**, 256801 (2002).

[14] P. Jarillo-Herrero, J.A. van Dam, and L.P. Kouwenhoven, Nature **439**, 953 (2006).

[15] N.M. Chtchelkatchev, G.B. Lesovik, and G. Blatter, Phys. Rev. B **62**, 3559 (2000).

[16] C.W.J. Beenakker, Phys. Rev. Lett. **67**, 3836 (1991).

[17] The quasiparticles spend a long time $\tau_{\text{dot}} \sim \hbar/\Gamma_n$ in the dot and only a short time $\tau_{\text{sc}} \sim \xi/v_{\text{F}} \sim \hbar/\Delta$ in the superconductor outside. Note that $q_{n,\text{eq}}^{\infty}$ starts to differ from $q_{n,\text{eq}}^{L/2}$ when $\delta\varepsilon_n > \Delta$, as the charge residing in the superconductor associated with $\varepsilon_n^{\text{A}} \approx \Delta$ is no longer small.

[18] D.A. Ivanov and M.V. Feigel'man, JETP Lett. **68**, 890 (1998).

[19] Three-dimensional phonon modes lead to rates suppressed by large factors $(\varepsilon/\hbar\omega_{\text{D}})^3(L/a) \sim 10^{-6}$ and $(\Delta/\hbar\omega_{\text{D}})^3(L/a) \sim 10^{-3}$, with ω_{D} the Debye frequency and we assume $\varepsilon/\hbar\omega_{\text{D}} \sim 10^{-3}$.

[20] A. Aassime, G. Johansson, G. Wendin, R.J. Schoelkopf, and P. Delsing, Phys. Rev. Lett. **86**, 3376 (2001).